IN-32
372702

The Implications of Encoder/Modulator/Phased Array Designs for Future Broadband LEO Communications.

Chris A. Jensen and John D. Terry*
Raytheon TI Systems, Inc, M.S. 8424, 6600 Chase Oaks Blvd Plano, TX, 75023.
Mark Vanderaar†‡
NYMA, Inc., 2001 Aerospace Parkway, Brookpark, OH, 44142.

October 3, 1997

ABSTRACT

In this paper we summarize the effects of modulation and channel coding on the design of wide angle scan, broadband, phased array antennas. In the paper we perform several trade studies. First, we investigate the amplifier back-off requirement as a function of variability of modulation envelope. Specifically, we contrast constant and non-constant envelope modulations, as well as single and multiple carrier schemes. Additionally, we address the issues and concerns of using pulse shaping filters with the above modulation types. Second, we quantify the effects of beam steering on the quality of data recovery using selected modulation techniques. In particular, we show that the frequency response of the array introduces intersymbol interference for broadband signals and that the mode of operation for the beam steering controller may introduce additional burst or random errors. Finally, we show that the encoder/modulator design must be performed in conjuction with the phased array antenna design.

Keywords: Intermodulation Distortion, Phase Array Antennas, NPR, Broadband Communications, Satellite Communications, LEO Constellation, Multi-beam Antenna

1 Introduction

In the past few years, a number of low earth orbiting (LEO) satellite constellation have been proposed, most of which will employ one or more multi-beam electronically scannable antenna arrays to provide next generation digital satellite service. The integration of high speed digital technology with electronically scanned antenna array technology is expected to revolutionize the satellite communication service – an industry which has historically lagged its terrestrial counterpart. Unfortunately, the integration of these two technologies also bring about a host – both new and old – of technological challenges for communication system engineers.

*C.A.J.: Email: chrisj@rtis.ray.com J.D.T.: .Email: j-terry1@rtis.ray.com
†M.V.: Email: mark.j.vanderaar@lerc.nasa.gov
‡Work supported by NASA Cooperative Agreement NCC3-497 "Direct Data Distribution System".

Many of the technical challenges have been addressed in the past with other satellites such as the age old problem of power limitations which require operation of transmit power amplifiers in nonlinear regions near saturation. In these regions, particular attention must be paid to amplitude and phase distortions. In the past, satellite repeaters for systems such as INTELSAT IV used high power travelling-wave tube (TWT) amplifiers which has since been replaced with solid-state power amplifier (SSPA). For both TWTs and SSPAs, the nonlinear distortions effects of amplitude modulation to amplitude modulation (AM/AM) and amplitude modulation to phase modulation (AM/PM) is present during near saturation operation. Significant effort in[1-5] has been made in attempting to develop analytic expressions that characterize these effects. A common approach employed, currently, to model these effects is to use bandpass nonlinearity; that is, a memoryless nonlinearity[3] sandwiched between band-pass filters (BPF) which is the approach taken in this paper. In this paper, the bandpass nonlinearity model is used to specify RF system performance criteria such as two-tone intermodulation (IMD) and noise power ratio (NPR). Further, it is used to assess the link performance by means of Monte Carlo simulations for those performance criteria mentioned. These Monte Carlo simulations are evaluated for single and multiple carrier configurations for candidate modulation schemes.

Other technical challenges result from stringent regulatory emission requirements to prevent interference with existing navigation communication and radio astronomy systems. These requirements, in addition to channel capacity issues, necessitate the use of the sharp roll-off filters such as square root-raised cosine and Gaussian filters. The introduction of filtering results in intersymbol interference (ISI) and envelope fluctuations of the transmitted signals. For linear channels, ISI is nearly eliminated using Nyquist shaping. In contrast, for nonlinear channels such as those created by nonlinear operation of the transmit amplifiers, ISI is always present and will eventually create serious problems at the receiver. In sections 3.1.2, simulation results illustrating this effects with the bandpass nonlinearity model fitted to measured data is presented.

Another sources of ISI for the system are found from the array group delay. The array group delay being defined as the time required for the signal to traverse across the array. The extent of these effects on the system performance bit error rate (BER) is investigated in this paper using a quaternary phase shift keying (QPSK) modulation scheme. Since the longest dimension of the antenna array is the limiting case, it is used in the simulation mentioned above.

In the final section of the paper, we introduce a distortion particular to the system considered and heretofore uncharacterized for satellite communication systems. Namely, we investigate the effects of the method of update by the beamsteering controller (BSC) for beam pointing during data transmission on the quality of data recovery. Very little has been reported on these effects in the literature, mainly, because the use of electronically scannable array antennas have been limited to the radar community where beam positions are updated between pulse transmissions. Unfortunately, this will most likely not be an option for these LEO based satellite systems since the beamwidths for these system will typically be less than a few degrees and require continuous beam tracking.

As a final remark before proceeding to the main body of this paper, throughout this document we will relate component or subsystem level tests to the overall system level BER performance – the most commonly used measure of performance for digital communications.

2 Data Model

In this section, we describe the mathematical model used to represent the propagating digital waveforms across the satellite link in the simulations. We begin with a description of the temporal portion of the waveform which has complex representation given by

$$s(t) = u(t)e^{-j2\pi f_c t} \tag{1}$$

where $u(t)$ represents the narrowband information bearing signal. Next, we incorporate the spatial aspects into the complex waveform model for a linear antenna array of isotropic elements. Consider the superposition of d digital signals and multipath reflections incident on an M sensor linear array. We assume the signal is corrupted by independent identically distributed spatiotemporal white Gaussian noise; thus, the output of the array is given by

$$\mathbf{y}(t) = \sum_{k=1}^{d} \gamma_k \mathbf{a}(\theta_k)\alpha_k s_k(t - \tau_k) + \mathbf{v}(t) \tag{2}$$

where γ_k is the amplitude of the kth signal, $\mathbf{a}(\theta_k)$ is the steering vector for a signal arriving from the direction θ_k, s_k is the kth signal waveform, τ_k is the delay associated with the kth signal, α_k is the attenuation associated with the kth signal, and $\mathbf{v}$ is additive white noise process. If we assume narrowband signals, then the time-delays can be modeled as phase-shifts. Hence, the baseband demodulated signal after match filtering can be written as

$$\mathbf{y}(m) = \sum_{k=1}^{d} \gamma_k \alpha_k e^{-j\omega_c \tau_k} \mathbf{a}(\theta_k) s_k(m) + \mathbf{v}(m), \qquad m = 0, \ldots, N-1 \tag{3}$$

At the earth ground terminal in the simulation, the received baseband signal, $r(m)$, is computed using

$$r(m) = \Re\left(\mathbf{w}^{\dagger}\mathbf{y}(m)\right) \tag{4}$$

where $\Re$ denotes the real part and $\mathbf{w}$ is an antenna aperture response vector for some assumed direction of arrival for the incoming signal of interest. For the Monte Carlo simulations, $r(m)$ is compared to a replica of the transmitted signal to compute the BER for the system.

3 System Impairments

In this section, we describe several component level distortions for the antenna subsystem and relate their individual effects on the overall BER performance for the forward link of a satellite system. These component level distortions for the antenna subsystem fall into three broad categories: amplifier nonlinearities, array group delay, and BSC errors.

3.1 Amplifier Nonlinearities

As was mentioned in the introduction, the use of solid-state power amplifiers (SSPA) in current phased array antenna design introduces nonlinearities into the signal path. These distortions results in AM/AM modulation of the envelope and AM/PM modulation of the phase of the signal described in (1) where the output power and input power are related by a curve as shown in Figure 1. There are several approximations in the literature for these distortions. For instance, modified Bessel functions can been used to model the nonlinearities.[2] A major advantage to using Bessel functions is that it tends to yield fewer coefficients for a least-squares fit to measured data compared to other approximations. Others[4-5] have opted to use polynomial approximations. This approximation is accurate within a certain range of input voltage. Unfortunately, anomalolies can result for very large values of the input voltage. To avoid this undesirable effect, the range of input voltages are segmented into overlapping regions over which piecewise polynomial fits to the AM/AM and AM/PM distortion is performed. For

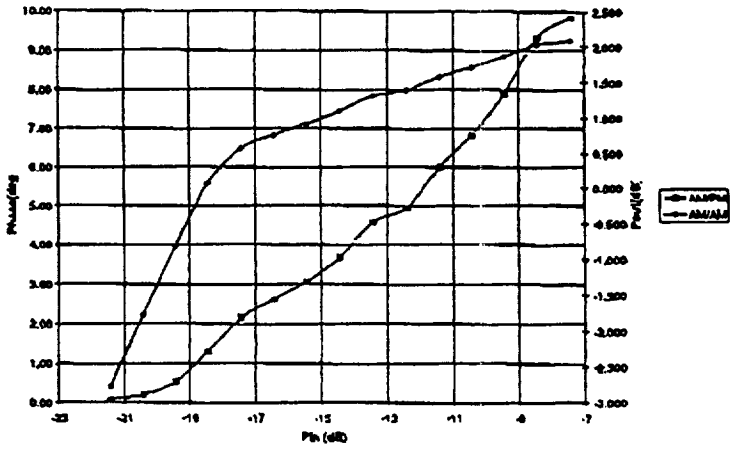

Figure 1: Power Transfer Characteristics for AM\AM and AM\PM Distortions

example, the AM/AM characteristics of a linear amplifier, $x(t)$, is well approximated in its linear region of operation by the cubic polynomial given below

$$x(t) = k_1 s(t) - k_3 s(t)^3 \tag{5}$$

where k_1 equals the linear voltage gain for the amplifier and k_3 is related to k_1 and the intercept point (IPi) for a two-tone stimulus test in accordance to

$$IPi = 10\log(\frac{2k_1^3}{3|k_3|}) \tag{6}$$

for an 1 Ω resistance. In contrast, the model does not predict the non-linearity distortions in the saturation region of an amplifier. A more appropriate model for the AM/AM characteristics in that region is a zero-memory non-linearity such as a limiter model; that is, a device which, as the input signal level is increased, limits the output signal level at some point. Even if the input signal level is further increased, the output voltage remains at this saturation level. The main cause of the limiting effect is due to the fixed supply for the amplifier. Although several limiter models have been proposed in the literature, the limiter model used in these simulations is

$$z(t) = \frac{L \cdot sgn(x(t))}{\left[1 + \left(\frac{L}{|x(t)|}\right)^s\right]^{1/s}} \tag{7}$$

where x is the instantaneous input voltage, z is the instantaneous output voltage, L is the asymptotic output level as $|x|$ approaches infinity, and s is the knee sharpness. The reason for choosing this particular limiter model is it has unity gain for small-scale signals, i.e. the linear region, and parameter controllable limiting characteristics for large scale signals. Similarly, we used piece-wise approximations for the AM/PM characteristics as well in the simulations. As an illustration, the power transfer characteristics of the amplifier model used throughout the simulations is shown in Figure 1. The effects of the AM/AM distortion of the amplifier on a quaternary phase shift keying (QPSK) signal is shown in Figure 2. We observe the net effect of the AM/AM distortion is to alternatively compress and expand the signal constellation which can have a severe effect on certain modulation schemes. In constrast, the net effect of the AM/PM distortion shown in Figure 3 results in a rotation of the signal constellation as a function of input power. Clearly, any coherently detected signal will suffer degradation in performance

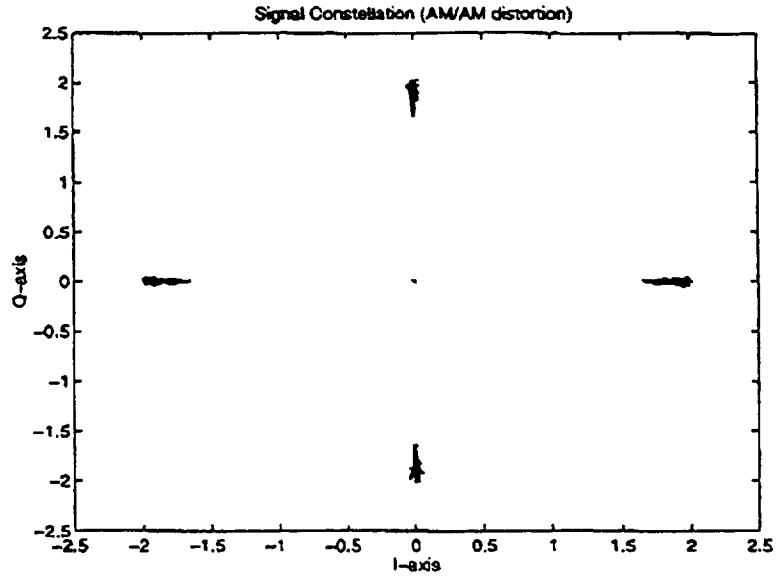

Figure 2: AM/AM Distortions of a QPSK Signal

due to this distortion. The combined effects of AM/AM and AM/PM degrades the performance of all digital communication signal of note.

To summarize, the benefit to using piecewise approximations is that it leads to better control and predictability of the IMD performance in addition to matching the AM/AM and AM/PM characteristics.

3.1.1 Performance Criteria

There are several performance metrics used to assess the behavior of an amplifier. Two common metrics are two-tone intermodulation distortion (IMD) and noise power ratio (NPR). The amount of distortion introduced determines how much the input drive power of the amplifier is backed off (iBO) from the saturation level.

IMD Two-tone intermodulation distortion (IMD) is a well-known and well-documented phenomenon. The equations for relating the IPi to intermodulation rejection (IMR) is as follows:

$$IMR = \frac{2}{3}(IPi - TonePwr + IMR) \quad (8)$$

$$\frac{1}{3}IMR = \frac{2}{3}(IPi - TonePwr) \quad (9)$$

$$IMR = 2(IPi - TonePwr) \quad (10)$$

where $TonePwr$ is the power in the tone. Note all quantities shown in (8)-(10) are in dB. Leffel[1] shows that the two-tone test can be used to predict multi-tone intermodulation performance. The analysis presented demonstrates the predictability of the level of IM in a linear device when subjected to more than two tones. However, this is not a worst case calculation, but rather the average if this same device

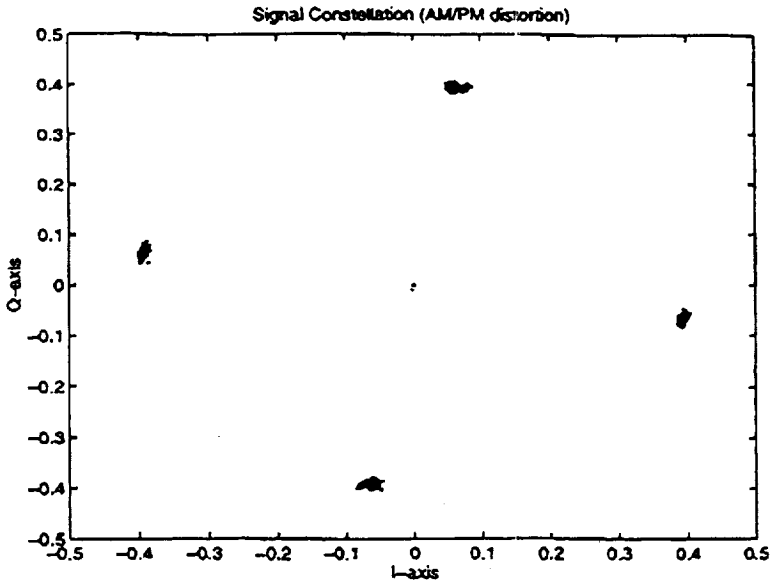

Figure 3: AM/PM Distortions of a QPSK Signal

were measured hundreds of times with the same set of tones, but different offset phases. A two-tone stimulus test for the saturation region of the amplifier model used in the simulations is shown in Figure 4.

NPR Noise Power Ratio (NPR) is criterion was developed for evaluation of SSPAs for telecommunications applications. The tests entails passing a signal with white noise like characteristics, from which a portion of the spectrum has been removed, through an amplifier under test. NPR is the ratio of the power of the spectral components in the pass band to power in the notch. To ensure the repeatability and accuracy of the test, one must take care in setting the parameters for the test. A list of the parameters needed to define the NPR stimulus and a brief description of each is given below:

- Average power – This is the total average power in the signal.
- Bandwidth Occupancy – This is the spectral extent of the signal for all components in the spectrum above a given power threshold.
- Bandwidth of Notch – The bandwidth of the notch should be sufficiently small such that the noiselike signal appears be to "flat" across the notch's bandwidth.
- Depth of Notch – The NPR of the stimulus should be 15 dB greater than the NPR of the amplifier to ensure an error less than 0.1 dB.
- Peak Value of the Noise Signal – This sets the peak value to the average value and is an indication of the "stress factor" of the stimulus.

An example of NPR measurement for the saturation region of operation is depicted in Figure 5. A final note concerning these performance metrics for the amplifier is that the response of each of the tests depends on the stimulus employed. To improve accuracy of Monte Carlo simulations, the data

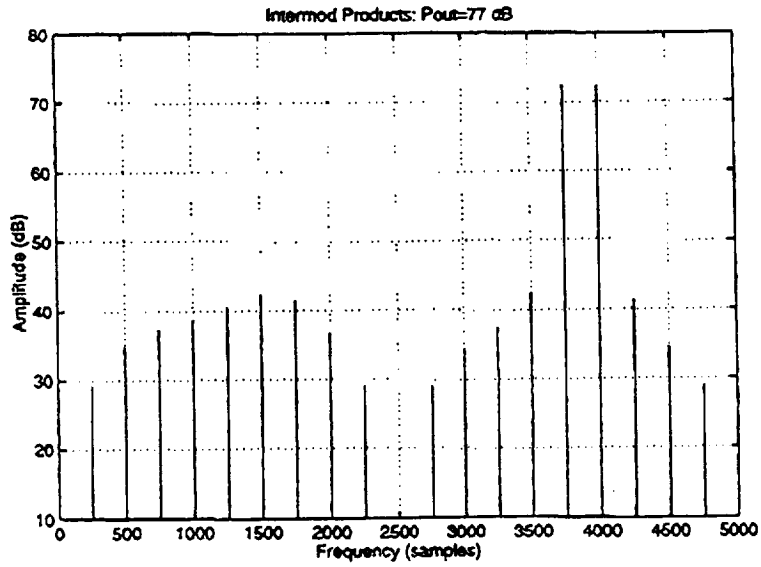

Figure 4: Two-Tone Intermodulation Distortions for the Saturation Region of the Amplifier

used to fit an amplifier's model needs to be measured with a test stimulus whose characteristics are very similar to the actual signal expected in the communication system.

3.1.2 Single Carrier Envelope Fluctuations

There are two sources of envelope fluctuations for a single carrier digital communication signal. One occurs for any digital communication signal whose envelope is non-constant. For those digital communication signals, the peak to average power is the figure of merit in terms of the amount of non-linearities introduced; that is, the larger the peak to average power, the greater the distortion on the signal waveform. The other occurs when filtering is introduced between the transmitter and receiver of the communication system. The effects of filtering results in waveform distortions and bit spreading. The former results in AM/AM and AM/PM distortions, and the latter, in intersymbol interference (ISI). In simulations, we examined these effects both individually and jointly. The functional block diagram of satellite communication system developed in Matlab®\Simulink® software is shown in Figure 6. To see the combined effects of filtering with the amplifier's non-linearities, we plotted the BER performance of a square root raised cosine filtered 16 QAM signal as a function of output drive level in Figure 7.

In Figure 7, the one dB compression point, P_{1dB}, for the amplifier is shown for reference. We observe that its value is approximately 1.1 dBW. We see from the graph that the performance of the output of the amplifier begins to slightly deviate from that of an ideal amplifier roughly 2 dB from the P_{1dB}. The ISI is the initial cause of this deviation; further along the curve, the AM/AM and AM/PM distortions begin to dominate the performance. This can be seen by noting the following. In accordance to (5), the degradation in the signal-to-noise ratio (SNR) is given by

$$SNR_{AMP} = SNR_{Ideal}(1 - \frac{k_3 P_s}{k_1}) \quad for \quad k_1 \gg k_3 P_s \tag{11}$$

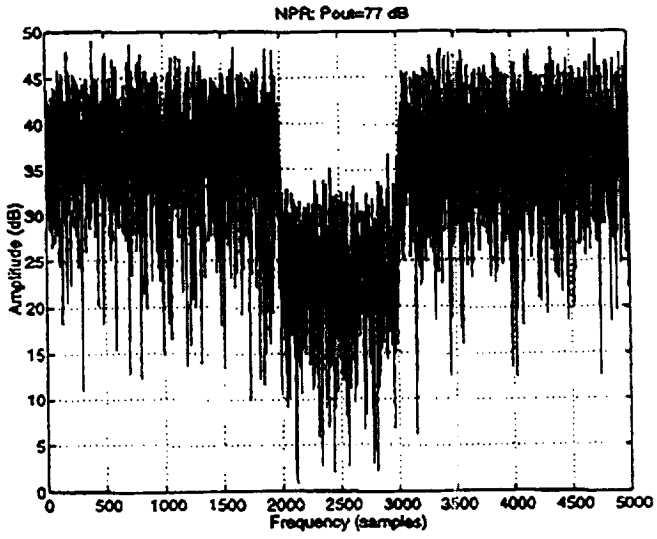

Figure 5: NPR for the Saturation Region of the Amplifier

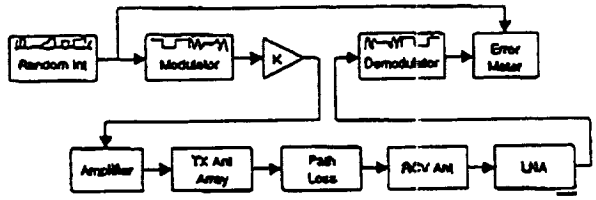

Figure 6: Functional Block Diagram of the Satellite Communication System

where in P_s is the power in the signal. In constrast, if the NPR is used as the performance metric, then the expected degradation in performance is slightly more complicated to compute. It is easily shown that the following relationship holds

$$\left(\frac{P_{MB}}{P_{SB}}\right)^{-1}_{Total} = \left(\frac{P_{MB}}{P_{SB}}\right)^{-1}_{Input} + NPR^{-1} \tag{12}$$

where P_{MB} is the power contained in the main beam bandwidth and P_{SB} is the power in the sidebands. The degradation is the reduction in P_{MB} from the input to the output of the amplifier. So, for inputs powers up to 2 dB below the P_{1dB}, the SNR degradation computed using (11) is less than 0.2 dB; in comparison, the SNR degradation is less than 0.14 dB assuming a P_{SB} equal to 1% of the total power and NPR equal to 14 dB as shown in 5.

Finally, the combination of spectrum shaping with a non-constant envelope has a poorer performance in terms of degradation from theoretical performance. Two final observations; first, to achieve near theoretical performance in saturation will require an iBO of 2-3 dB; and second, in the absence of iBO and the rest of the systems remaining the same, there is an absolute best performance the communication system can achieve which can be an order of magnitude worse than what is expected

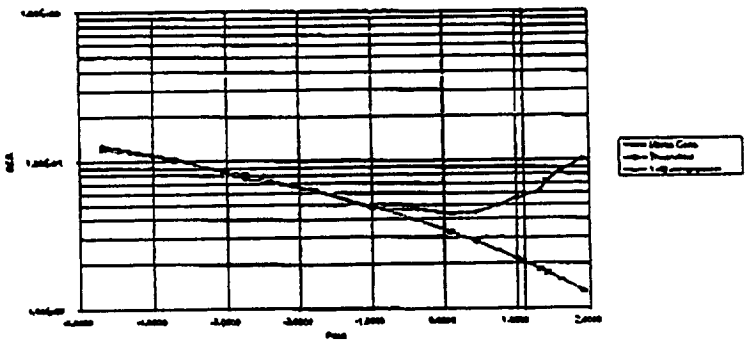

Figure 7: BER versus Output Drive Level Plot for Shaped 16 QAM Signal

for that power level. This phenomenon is readily visible from inspection of the graphs in Figure 7 when the signal is well into the saturation region.

3.1.3 Multiple Carrier Envelope Fluctuations

The addition of modulated carriers to the input signal of the amplifier increases the peak to average ratio and hence suffers greater degradation in performance compared to a single carrier. For example, the number of modulated carriers were increased from one to four and the resulting BER performances for the modulation schemes considered for the single carrier case is shown in Figure 8.We purposely combined the performances for the two inside and outside carriers for two reasons. One, it is makes the graph more readable and two, it allows us to note the additional degradation to adjacent channel interference (ACI) due to regrowth of the sidelobes for the modulated carriers. Notice that the ACI for the inside carriers is greater than those for the outside carriers since they each have two adjacent channel compared to an single adjacent channel for the outside carriers. Hence the appropriate performance metric should be the NPR. For each carrier, the two constituent components of degradation are the percentage loss of main lobe power and ACI due to the other carriers. Equation 12 is still valid here; however, P_{SB} has contributions from other carriers as well. The ACI, on the other hand, effects the net SNR ratio or the signal-to-noise pluse interference ratio SINR as follows

$$SINR^{-1} = ACI^{-1} + SNR^{-1} \tag{13}$$

As was noted in the previous section, near theoretical performance is achievable only when several dB of iBO is used. Here the iBO is 7.5-8 dB for four shaped 16 QAM signals.

3.2 Array Group Delay

The spacing of the antenna elements, the size of the antenna and the steering vector used to combine these elements cause variation in the frequency response over the information bandwidth, such that the frequency response is not flat over this bandwidth. Moreover, the situation worsens as the beam is steered away from the observer. Antenna engineers will recognize these effects as the result of frequency scanning the phased array. The effects of the frequency response of the array is intersymbol interference which degrades the system performance.

The array geometry model was developed using plane waves to compute the array response vector.

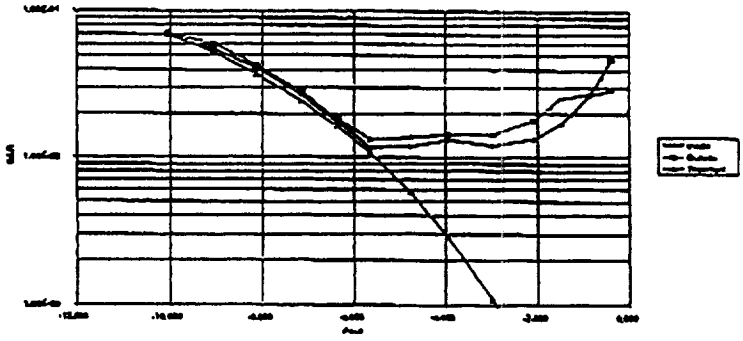

Figure 8: BER Performance versus Output Drive Level for four 16 QAM Signals.

This model is fairly accurate for narrowband signals whose inverse bandwidths are much greater than the time required to traverse across the array. However, for wide band signals, the validity of the model no longer holds. In this case, we used time domain modeling to accurately account for the time dispersion or bit spreading due to the array group delay. A mathematical expression used to predict this phenomenon for a rectangular planar array is

$$|AF(\theta,\phi,f)| = \frac{1}{N_x N_y} \frac{\sin\left(N_x \Psi(\theta,\phi,f)/2\right) \cdot \sin\left(N_x X(\theta,\phi,f)/2\right)}{\sin\left(\Psi(\theta,\phi,f)/2\right) \cdot \sin\left(X(\theta,\phi,f)/2\right)} \tag{14}$$

where

$$\begin{aligned} \Psi(\theta,\phi,f) &= \frac{2\pi\Delta_x}{c}\left(f\sin(\theta_o)\cos(\theta_o) - f_c\sin(\theta_s)\cos(\theta_s)\right) \\ X(\theta,\phi,f) &= \frac{2\pi\Delta_y}{c}\left(f\sin(\theta_o)\sin(\theta_o) - f_c\sin(\theta_s)\sin(\theta_s)\right) \end{aligned} \tag{15}$$

Here the subscripts c, o and s denote carrier, observer and scan; N_x and N_y are the number of elements in the x and y directions; Δ_x and Δ_y are the spacing in the x and y directions for the array; and θ and ϕ are the azimuth and elevation angles. Last, $|AF|$ is the magnitude response of the array. For an arbitrary array geometry, complex exponentials, whose arguments are given in 15, are summed over the aperture of the array to compute $|AF|$. The effects of this frequency dependent response of array is the introduction of ISI. To qualify this effect, we observe in Figure 9 the degradation in BER as the instantaneous bandwidth of the information signal is increased. Around 933 MHz and 1244 MHz, the loss caused by ISI is approximately 0.2 dB. At 1866 MHz, the loss has increased to approximately 0.45 dB which is significant and continues to increase rapidly as the bandwidth is expanded. We note from the graph that ISI becomes significant when the time required to travel the longest dimension of the array is 1.6 times the inverse of the instantaneous bandwidth. When the ISI becomes too severe, this will necessitate the incorporation of an equalizer in the encoder/modulator design.

3.3 Phase Shifter Induced Errors

Recall that a key issue to be addressed in this paper was the effects of beamsteering on the quality of data recovery. We wanted to quantify the amount and type of distortions introduced by the phase shifters. The two modes of operation considered here are parallel and series update. For parallel update, all the phase shifters are updated simultaneously. For the series update, each phase shifter is updated one at a time until the array has been steered to its new location.

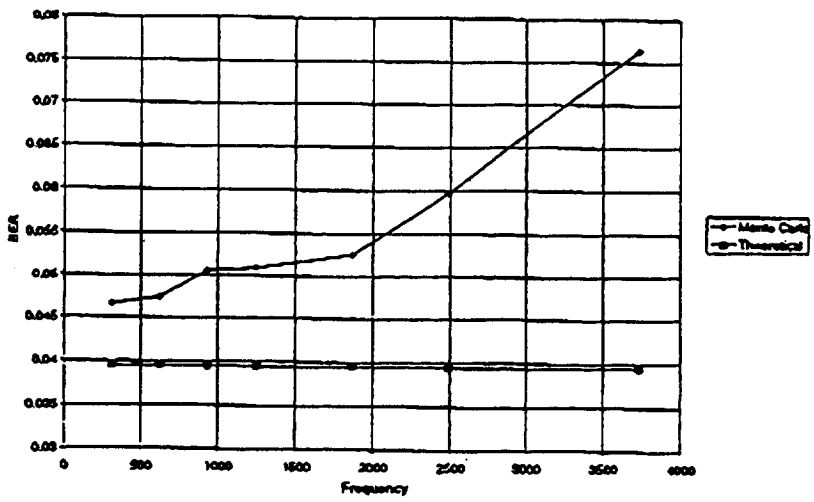

Figure 9: BER Degradation Due to Array Group Delay.

Burst Duration	BER	Average No. Errors/Burst
8 ns	4.9e-4	0.333
16 ns	7.82e-4	1.000
64 ns	1.5e-3	8.333
256 ns	1.5e-3	32.53

Table 1: Parallel Update Mode BER Performance

For switched line phase shifters, a good approximation of its transient reponse for amplitude and phase during switching is an N-bit quantizer followed by a secord order loop filter. The phase response of the phase shifters is obtained from the unit step response of the filter for each new phase setting. The amplitude response of the phase shifter is modeled as an attenuation notch of varied duration. The filter parameters, such as mean peak overshoot, rise and settle times, were determined from measured data of actual phase shifters. In the simulation, we read from a matrix the pre-computed time domain response of the filter for each element of the array for some assumed phase profile. The array gain response at each sampling instant is computed for a particular look direction using the phase shifter value for that instant.

In the simulation, the series update mode did result in a very slight loss due to beam broadening during the intermediate state between beam positions. However, there were no noticeable effects on the BER performance. In fact, the beam broadening due to series update mode lead to only 0.07 dB loss at 15° scanned off of boresight.

The parallel update model introduced burst errors. The number of errors introduced depended on the duration of the notch for the amplitude response of the phase shifter. Table 1 summarizes the finding of the simulations.

What one should take from these results are that although there is clearly degradation in performance due to the parallel updating of the phase shifter, the duration of the notch needs to be on the order of five times as large as the bit duration to average just a single bit error per burst. The update rate for the beam position and the transmitted data rate will determine if this has any significant effect on meeting the uncoded BER performance of the system. If this is the case, then the appropriate

channel coding needs to be employed to mitigate these effects.

4 Conclusions

In this paper, we presented several new expressions for relating the system impairments of the phase array antenna subsystem on its BER performance. In particular, we reviewed some common definitions for amplifier performance metrics such as IMD and NPR. Next for a single modulated carrier, we provided, heretofore unreported, relationships between the aforementioned metrics and the resulting BER performance for up to near saturation operation of a transmit power amplifier. In the following section, we showed a straightforward extension for multiple modulated carriers, hence enabling the communication system engineer to appropriately budget those losses for link analysis. We concluded the section by noting, for the systems considered, iBOs of several dB are required for near theoretical performance. In the absense of iBO, the system performance will be limited to some best performance independent of the amount of input drive power to the amplifier.

The other system impairment considered in this paper characterized the effects of beamsteering on the quality of data recovery. These can be divided into two major categories: array group delay and phase shifter update. For array group delay, it was noted that the use of phase shift to model time delay yielded ISI on the information signal. For phase shifter update, the type and quantity of errors introduced for the two modes of operation for the phase shifter were presented. It was found that a series update of the phase shifters lead to negligible degradation in performance while the parallel update mode yielded burst errors. We also report the conditions for which each of these distortions become significant and their impact on the encoder/modulator design.

The overall theme illustrated throughout this paper is that the design of the encoder/modulator and phased array antennas system must be performed in conjunction rather than separately as has been done historically.

5 REFERENCES

[1] M. Leffel, "Intermodulation distortion in a multi-signal environment," *RF Design Magazine*, June, 1995.

[2] P. Hetrakul and D. P. Taylor, "The effects of transponder non-linearity on binary CPSK signal transmission", *IEEE Trans. Commun.*, vol. COM-24, May 1976, pp. 546-553.

[3] R. G. Lyons, "The effect of bandpass non-linearity on signal detectability", *IEEE Trans. Commun. Technol.*, vol. COM-21, Jan. 1973, pp. 51-60.

[4] D. Schick, "Use peak factor to characterize power amplifiers", *Microwave & RF Magazine*, July 1997.

[5] S. Chen, W. Panton, and R. Gilmore, "Effects of Nonlinear distortion on CDMA communication systems", *IEEE Trans. on Microwave Theory and Techniques*, vol. 44, no. 12, December 1996.

[6] J. J. Jones, "Filter distortion and intersymbol interference on PSK signals", *IEEE Trans. Commun.*, vol. COM-19, April 1971, pp. 120-132.

[7] V. K. Bhargava, D. Haccoun, R. Matyas, and P. P. Nuspl, *Digital Communications by Satellite: Modulation, Multiple Access, and Coding*. Krieger Publishing Company, 1991.